Analysis of solids with different matrices by buffer-gas-assisted laser ionization orthogonal time-of-flight mass spectrometry

Quan Yu,[a] Lingfeng Li,[a] Eryi Zhu,[a] Wei Hang,*[ab] Jian He[c] and Benli Huang[a]

Received 12th January 2010, Accepted 14th April 2010
First published as an Advance Article on the web 6th May 2010
DOI: 10.1039/c000633e

A laser ionization orthogonal time-of-flight mass spectrometer with a low-pressure source and high laser irradiance was used to analyze 27 solid samples with 9 different matrices, including aluminium, soil, copper sulfide, zinc sulfide, iron, nickel, copper, zinc, and tungsten. The influence of laser energy on non-stoichiometric effects, such as matrix effects and elemental fractionation, has been investigated. The results indicate that matrix effects can be alleviated to a great extent at high laser irradiance. Additionally, with the irradiance of 10^{10}–10^{11} W cm^{-2}, most elements presented relatively stable relative sensitivity coefficients (RSC), while W, Pb, and Bi demonstrated unusual characteristics that their RSCs increased along with increasing laser energy.

Introduction

The laser sampling technique in atomic spectrometry provides a rapid and sensitive method for elemental determination for solid samples.[1,2] However, lots of previous studies show that the laser-solid interaction suffers from the problems of matrix effects and elemental fractionation, both of which limit the quantitative capability of laser-drive techniques such as laser ablation inductively coupled mass spectrometry (LA-ICPMS), laser-induced breakdown spectroscopy (LIBS), and laser ionization mass spectrometry (LIMS).[3–6] For example, during the laser sampling process, the fractionation is found as a function of laser properties like wavelength, pulse duration, power density, and even the repetition rate.[7–10]

Laser sampling techniques have vast applications in current analytical field; thus, improving the accuracy in quantitative analysis is worth extensive investigation. Various strategies have been developed to solve the problems of matrix effects and elemental fractionation in the LA-ICPMS field.[11–16] However, such of the studies are rarely carried out in LIMS. LIMS is based on the analysis of ions from laser plasma that present the chemical composition of the sample material.[17–19] Its accuracy depends not only on the instrumental capabilities but also on the elemental sensitivity in the whole measurement procedure, including the ablation/ionization process, ion transmission, and detection processes. Unlike the LA-ICPMS system, in which laser ablation, aerosol transportation, and ICP ionization are separated processes, LIMS combines the ablation and ionization into one process.[19,20] Hence the routinely used power density in LIMS was in the range of 10^{9}–10^{11} W cm^{-2} to produce sufficient ions for mass spectrometry analysis, which is generally larger than that for LA-ICPMS or LIBS.[19,21] Although increasing laser power can reduce elemental fractionation, a significant population of multi-charged ions will also be generated, resulting in severe spectral interference.[21,22] From our previous studies, the injection of inert gas in the ion source is proved to be a successful strategy to suppress the interference of multiply charged ions without losing useful analytical signals.[21,23] On the basis of the preliminary works, a comprehensive analysis of solids by LI-O-TOFMS has been performed for various samples with different matrixes, including alloys, ores, and sulfides. The applied laser irradiance flux covered three orders of magnitude to examine the influence of the laser energy on experimental results.

Experiment

All the experiments were carried out on an in-house built LI-O-TOFMS system that has been described previously with only a few modifications.[24,25] Briefly, a Nd:YAG laser (NL303G, EKSPLA) was used operating at duration of 4.4 ns and wavelength of 355 nm, with variable pulse energies ranging from 0.04 to 9.6 mJ. The focal spot was about 20 μm in diameter. Ultrahigh purity helium was introduced into the ion source with a pressure of 500 Pa. In the TOF analyzer, the orthogonal accelerator operated in a "pulse train" mode.[23] The pulse has a frequency of 33 kHz and starts at a delay time of 100 μs after the laser pulse. A digital storage oscilloscope (42Xs, 2.5 Gs s^{-1}, Lecroy) was used for signal acquisition instead of the time-to-digital converter used previously.[24] With this setup, it takes 10 s to acquire each integrated spectrum with laser pulse frequency at 10 Hz. Two M-661 miniature translation stages (Physik Instrumente Co.) were stacked to act as a two-dimensional manipulator with a moving frequency of 1 Hz and a distance of 200 μm/step for fresh sample surface.

The standards used in this study were obtained from National Institute of Standards and Technology and Chinese National Standards. The investigation was performed on the analysis of 27 solid samples including 9 matrices: aluminium (GBW E921b, GBW E922b, GBW E923b, GBW E926a), soil (GBW (E)070043, GBW (E)070045, GBW 07123), iron (SRM 1762, GBW 01396, GBW 01398, GBW01399, GBW01400, GSBH-40115-2,

[a]*Department of Chemistry, Key Laboratory of Analytical Sciences, College of Chemistry and Chemical Engineering, Xiamen University, Xiamen, 361005, China. E-mail: weihang@xmu.edu.cn*
[b]*State Key Laboratory of Marine Environmental Science, Xiamen University, Xiamen, 361005, China*
[c]*Department of Mechanical and Electrical Engineering, Xiamen University, Xiamen, 361005, China*

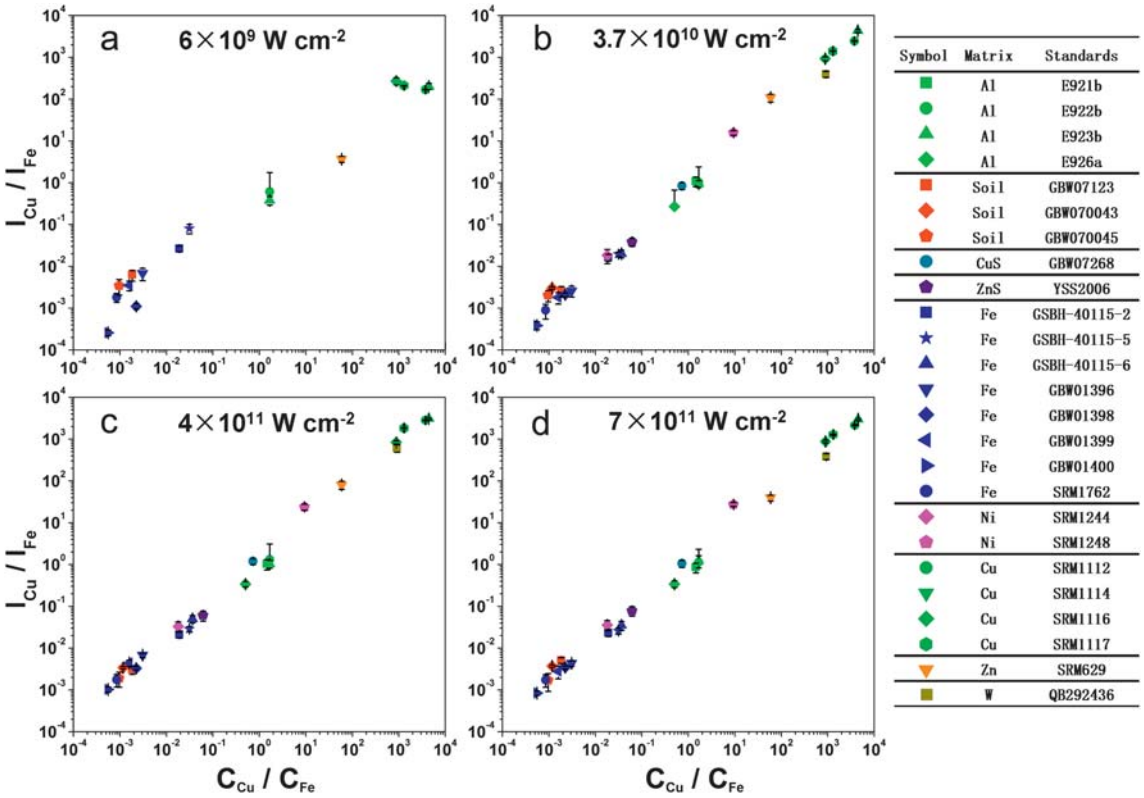

Fig. 1 Logarithmic plot showing the ratio of intensities as a function of ratio of elemental compositions in the presence of different matrices and at different irradiances.

GSBH-40115-5, GSBH-40115-6), zinc sulfide (GBW YSS2006), copper sulfide (GBW 07268), copper (SRM 1112, SRM 1114, SRM 1116, SRM 1117), nickel (SRM 1244, SRM C1248), zinc (SRM 629), and tungsten (GBW QB200335, GBW QB337618, GBW QB292436). All the samples were treated following the same procedure as in previous experiments[24] that the alloys were cut into discs of 6 mm in diameter and 1.5 mm in thickness, whereas the powder samples were pressed into the same shapes as the alloy discs.

Results and discussion

The influence of matrix effects is the main reason that limits laser sampling techniques in quantitative analysis.[2] For instance, matrix-matched calibration standards are required in routine quantitative analysis using LA-ICPMS, interested elements should be contained in the standards and within the suitable concentration range. These standards are commonly costly and hard to find or fabricate. Some previous works in our instrument have proved the feasibility of quantitative analysis for solid samples by LI-O-TOFMS.[23,26] The current investigation has further validated the conclusion by the experiments on various samples of different matrices. As shown in Fig. 1, responses of ion signal *versus* elemental contents in different samples were used to evaluate the matrix effects. In order to eliminate the source fluctuation and instrument shift, Fe was selected as the internal reference element considering its existence in all standards in the experiment.

As shown in Fig. 1a, at low laser irradiance ($\sim 10^9$ W cm^{-2}), the analytical result was affected by the sample matrix. The response between signal intensities and elemental concentrations was clearly different for the samples of different matrices. However, the influence of matrix effect was mitigated when increasing the laser energy, indicated by the improved uniformity of the signal-concentration responses in Fig. 1b, 1c, and 1d. Similar phenomena were also observed for other elements. Matrix composition may influence the early stage of laser-solid interaction, including mass melting, sublimation or vaporization.

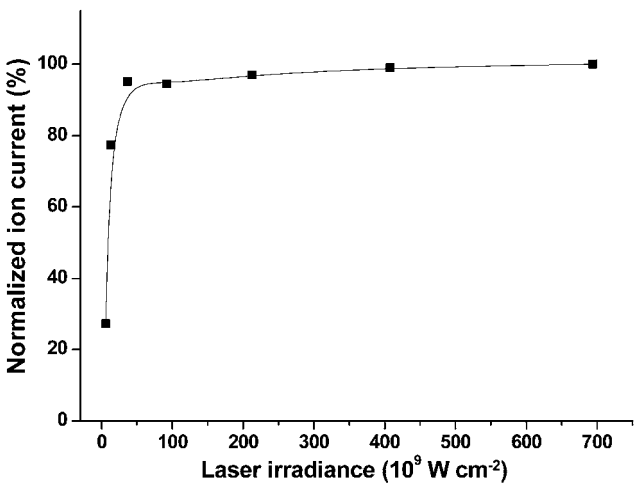

Fig. 2 Plot of the total ion current (TIC) *versus* laser irradiance. The sample studied was SRM C1248 alloy.

However, the high irradiance creates extremely hot plasma greatly exceeding the vaporization temperature of most materials; the diversity of thermal properties among different matrices is minimized in the laser ablation and atomization processes. Ionization at high irradiance is achieved through multiple mechanisms including thermal ionization, impact ionization, and multiphoton ionization.[27,28] Theoretically, there should be no matrix-related effects occurring during these ionization processes. As a result, matrix effect can be largely eliminated at high laser irradiance.

It is obvious that high irradiance will result in high ion productions in laser ionization. In our buffer-gas-assisted ion source TOFMS, the total ion current approached a saturated level as the laser energy increased (see Fig. 2), which could be caused by the space charge effect when the ion beam was passing through the nozzle. A mass spectrometer, including the transmission system, mass analyzer, and the detection system, may response nonlinearly to the variable ion current. Once the current reached the saturated level, the system can be optimized for the "fixed" current, and response steadily, which is independent of the laser irradiance. As shown in Fig. 1b, 1c, and 1d, the analytical results under different high irradiances present similar characteristics.

In the application of solid analysis, elemental fractionation was another important factor that should be concerned about. This effect can be evaluated by the relative sensitivity coefficient (RSC), which is proposed to be a function of the physical and chemical properties of sample.[17] It is found that the fractionation was generally influenced by the parameters of the laser, wherein, laser pulse energy was always considered as the most important factor that moderately increasing the laser irradiance, especially in the range of 10^9–10^{10} W cm^{-2}, can facilitate the reduction of fractionation.[7,17,19,21] In order to evaluate the fractionation, the RSCs of all elements of interest acquired under the irradiance of 9×10^{10} W cm^{-2} were listed in Table 1. It can be seen that, under high laser irradiance, the RSC variations among different matrices are averaged at 16% for all elements studied, and within 30% for most elements except Al and Zr.

In addition, the influence of irradiance on elemental RSCs has also been investigated, and the result of representative elements was shown in Fig. 3. Although fractionation could still be observed at high irradiance, most elements, including the elements not shown in Fig. 3, have relatively stable RSCs in the presence of variable laser energies. W, Pb, and Bi show different characteristics that their RSCs were increased along with the increasing irradiance. Since the lattice-heat diffusion must be taken into account in nanosecond laser ablation, the adjacent material surface of the crater is also melt and vaporized.[29] In comparison with the mass removal in the laser radiation area, this heat diffusion vaporization is related to the melting point (MP) and boiling point (BP) of the element since the temperature in the heat-diffused zone is much less than that in laser radiation area. Hence, elements with low MP and BP (such as Pb and Bi) may have enhanced compositions in the vaporized mass plume. This fractionation will be significantly enhanced in high irradiance laser radiation, owing to the extended heat-diffused zone.

Table 1 RSC values determined from different matrices using LI-O-TOFMS at an irradiance of 9×10^{10} W cm^{-2}

Element	Relative sensitivity coefficients (RSC, x/Fe) for different matrices listed below									RSC variation among different matrices
	Soil	CuS	ZnS	Cu	Ni	Fe	Zn	Al	W	
Na	0.45 ± 0.03									—
Mg	0.15 ± 0.12						0.22	0.42 ± 0.06		53.2%
Al	0.28 ± 0.09				0.37 ± 0.01	0.43 ± 0.14	0.22	0.33 ± 0.07	0.40	23.1%
K	0.98 ± 0.14									—
Ca	0.31 ± 0.03									—
Ti	0.33 ± 0.04				0.40	0.29 ± 0.05		0.36 ± 0.06		13.5%
V	0.82					0.77 ± 0.06				4.4%
Cr	1.27				1.12 ± 0.11	1.09 ± 0.36	1.16			6.8%
Mn	1.00 ± 0.36	1.29			1.10 ± 0.14	1.11 ± 0.09		1.36 ± 0.28		12.6%
Ni				1.01 ± 0.18	1.02 ± 0.05	1.08 ± 0.21	0.87	1.18 ± 0.09	0.81 ± 0.24	13.6%
Co	1.24	1.25			1.28	1.36 ± 0.04				4.2%
Cu	1.25	1.43	1.22	1.07 ± 0.07	1.05 ± 0.16	1.21 ± 0.21	0.72	0.69 ± 0.13	0.93	23.3%
Zn	0.79 ± 0.15		1.09	0.74 ± 0.17	1.21 ± 0.08		0.67	0.92 ± 0.27		23.4%
Se		1.22								—
Rb	1.58 ± 0.38									—
Sr	1.34 ± 0.20									—
Zr[a]	0.96 ± 0.19					0.60 ± 0.19				32.6%
Nb[a]	0.70				0.86	0.70 ± 0.20				12.3%
Mo					1.80 ± 0.01	1.62 ± 0.63				7.4%
Ag		1.9	2.23							11.3%
Cd			2.50							—
Sn				1.23 ± 0.21		1.87 ± 0.29	1.27	2.13 ± 0.26		27.4%
Sb			2.18			1.92 ± 0.48				8.9%
Ba	2.43 ± 0.27									—
Ta						2.31				—
W						0.84 ± 0.11			0.80 ± 0.10	3.5%
Pb	2.69	3.04	2.52	2.68 ± 0.28	3.09	1.96 ± 0.14	2.76	2.71 ± 0.21		12.9%
Bi			3.12			2.47 ± 0.60				16.4%

[a] Sum intensity of singly charged ions and oxidation ions was used for the RSC calculation.

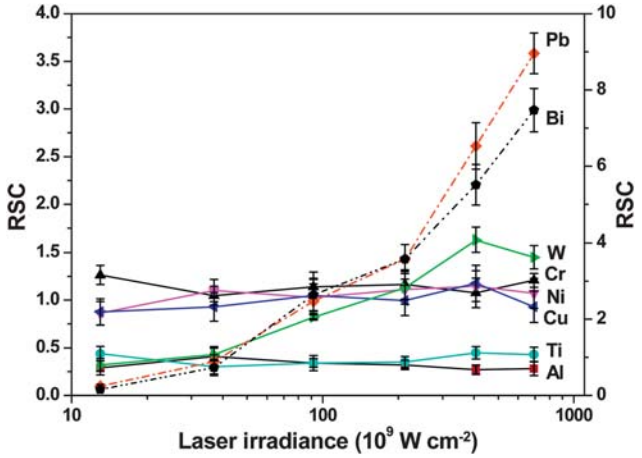

Fig. 3 Dependence of RSC values on laser irradiance for representative elements. RSCs of Al, Ti, Cr, Ni, Cu, and W refer to the left axis (from 0 to 4), and RSCs of Pb and Bi refer to the right axis (from 0 to 10). Error bars represent the RSC variations among different matrices.

The RSC of W increased at a slower rate compared with that of Pb and Bi; however, the reason for its enhancement with the laser irradiance is still unclear.

Conclusions

Based on current set-up of LI-O-TOFMS, rapid analysis of solid samples can be achieved. The ions sampled into the nozzle reach a saturated level with the increase of laser irradiance, which could simplify the optimization process and make the instrumental response independent of the irradiance. Under high laser irradiance ($\geq 10^{10}$ W cm^{-2}), matrix effects can be largely eliminated. Variation of laser irradiance has little influence on RSC values for most elements, except W, Pb, and Bi. The RSC variations among different matrices are averaged at 16% for all elements involved in this study. By solving the problems of multi-charged ion interference and large ion kinetic energy distribution, applying high laser irradiance is beneficial in many aspects for laser ionization mass spectrometry, and could be an effective solution to the problem of non-stoichiometric effects in laser-related techniques for solid analysis.

Acknowledgements

Financial support from the National 863 program, Natural Science Foundation of China, and Fujian Province Department of Science & Technology is gratefully acknowledged.

Reference

1 D. Gunther and B. Hattendorf, *Trends Anal. Chem.*, 2005, **24**(3), 255–265.
2 R. E. Russo, X. Mao and O. V. Borisov, *Trends Anal. Chem.*, 1998, **17**(8–9), 461–469.
3 D. Gunther, *Anal. Bioanal. Chem.*, 2002, **372**(1), 31–32.
4 J. D. Winefordner, I. B. Gornushkin, T. Correll, E. Gibb, B. W. Smith and N. Omenetto, *J. Anal. At. Spectrom.*, 2004, **19**(9), 1061–1083.
5 G. I. Ramendik, O. I. Kryuchkova, D. A. Tyurin, T. R. McHedlidze and M. S. Kaviladze, *Int. J. Mass Spectrom. Ion Processes*, 1985, **63**(1), 1–15.
6 D. Gunther, S. E. Jackson and H. P. Longerich, *Spectrochim. Acta, Part B*, 1999, **54**(3–4), 381–409.
7 R. E. Russo, X. L. Mao and S. S. Mao, *Anal. Chem.*, 2002, **74**(3), 70 A–77 A.
8 F. Claverie, B. Fernandez, C. Pecheyran, J. Alexis and O. F. X. Donard, *J. Anal. At. Spectrom.*, 2009, **24**(7), 891–902.
9 D. Gunther and C. A. Heinrich, *J. Anal. At. Spectrom.*, 1999, **14**(9), 1369–1374.
10 I. Kroslakova and D. Gunther, *J. Anal. At. Spectrom.*, 2007, **22**(1), 51–62.
11 J. Pisonero, B. Fernandez and D. Gunther, *J. Anal. At. Spectrom.*, 2009, **24**(9), 1145–1160.
12 R. E. Russo, X. Mao, J. J. Gonzalez and S. S. Mao, *J. Anal. At. Spectrom.*, 2002, **17**(9), 1072–1075.
13 J. Koch, M. Walle, J. Pisonero and D. Gunther, *J. Anal. At. Spectrom.*, 2006, **21**(9), 932–940.
14 B. Fernandez, F. Claverie, C. Pecheyran and O. F. X. Donard, *Trends Anal. Chem.*, 2007, **26**(10), 951–966.
15 M. L. Alexander, M. R. Smith, J. S. Hartman, A. Mendoza and D. W. Koppenaal, *Appl. Surf. Sci.*, 1998, **127–129**, 255–261.
16 M. Gaboardi and M. Humayun, *J. Anal. At. Spectrom.*, 2009, **24**(9), 1188–1197.
17 J. S. Becker and H. J. Dietze, *Fresenius J. Anal. Chem.*, 1992, **344**(3), 69–86.
18 Q. Yu, L. Chen, R. Huang, W. Hang, J. He and B. Huang, *Trends Anal. Chem.*, 2009, **28**(10), 1174–1185.
19 A. Vertes, R. Gijbels and F. Adams, ed., *Laser Ionization Mass Analysis*, Wiley-Interscience, New York. 1993.
20 A. A. Sysoev and A. A. Sysoev, *Eur. J. Mass Spectrom.*, 2002, **8**(3), 213–232.
21 W. Hang, *J. Anal. At. Spectrom.*, 2005, **20**(4), 301–307.
22 S. Kondrashev, T. Kanesue, M. Okamura and K. Sakakibara, *J. Appl. Phys.*, 2006, **100**(10), 103301–103308.
23 Q. Yu, R. Huang, L. Li, L. Lin, W. Hang, J. He and B. Huang, *Anal. Chem.*, 2009, **81**(11), 4343–4348.
24 J. He, R. Huang, Q. Yu, Y. Lin, W. Hang and B. Huang, *J. Mass Spectrom.*, 2009, **44**(5), 780–785.
25 R. Huang, Q. Yu, Q. Tong, W. Hang, J. He and B. Huang, *Spectrochim. Acta, Part B*, 2009, **64**(3), 255–261.
26 Q. Tong, Q. Yu, X. Jin, J. He, W. Hang and B. Huang, *J. Anal. At. Spectrom.*, 2009, **24**(2), 228–231.
27 J. P. Singh and S. N. Thakur, ed., *Laser-Induced Breakdown Spectroscopy* Elsevier, Oxford. 2007.
28 S. S. Harilal, C. V. Bindhu, R. C. Issac, V. P. N. Nampoori and C. P. G. Vallabhan, *J. Appl. Phys.*, 1997, **82**(5), 2140–2146.
29 R. Hergenroder, O. Samek and V. Hommes, *Mass Spectrom. Rev.*, 2006, **25**(4), 551–572.

